Quantum analogue of the Kolmogorov–Arnold–Moser transition in field-induced barrier penetration in a quartic potential

P. K. Chattaraj*, S. Sengupta, B. Maiti and U. Sarkar
Department of Chemistry, Indian Institute of Technology, Kharagpur 721 302, India

Quantum signatures of the Kolmogorov–Arnold–Moser (KAM) transition from the regular to chaotic classical dynamics of a double-well oscillator in the presence of an external monochromatic field of different amplitudes are analysed in terms of the corresponding Bohmian trajectories. It is observed that the classical chaos generally enhances the quantum fluctuations, while the quantum nonclassical effects try to suppress classical stochasticity.

THE study of quantum domain behaviour of classically chaotic systems has seen an upsurge of interest in recent years[1–21]. It has been shown that the classical stochasticity enhances the quantum fluctuations, while the quantum nonclassical effects tend to suppress classical chaos[1–20]. An invariant Kolmogorov–Arnold–Moser (KAM) torus characterizes an integrable classical system in the presence of a weak perturbation. If the strength of the external destabilizing field is increased[19], the phase space reveals chaotic dynamics as the sufficiently irrational KAM tori break down into cantori[20], so that the corresponding quantum system gets stabilized[16–18]. In order to have a better understanding of these aspects we study in the present work, the quantum signature of the classical chaos in a double-well oscillator in the presence of an external monochromatic field of varying intensity. This problem has been studied in detail in recent years[16–19] because of its importance in several areas of chemical dynamics[21]. In this case, the classical chaos and quantum tunnelling occur simultaneously to give rise to the coherent oscillatory nature of the quantum diffusion between two stable KAM tori.

Description of classically chaotic systems in the quantum domain has been studied successfully[1–21] using quantum potential-based theories like quantum fluid dynamics (QFD)[22] and quantum theory of motion (QTM)[12]. In QFD[22], the quantum dynamics is understood in terms of the motion of a probability fluid having density $\rho(\mathbf{r}, t)$ and velocity $\upsilon(\mathbf{r}, t)$ moving under the influence of the external classical potential augmented by a quantum potential. An equation of continuity and an Euler-type equation of motion comprise the fundamental equations of QFD[22]. These equations can be written[10] in the form of Hamilton's equations of motion with a properly defined Hamiltonian functional and by considering $\rho(\mathbf{r}, t)$ and $(-\chi(\mathbf{r}, t))$ as canonically conjugate variables, $\chi(\mathbf{r}, t)$ being the velocity potential ($\upsilon(\mathbf{r}, t) = \nabla\chi(\mathbf{r}, t)$). Quantum chaos in a Henon–Heiles oscillator has been studied[10] through $\rho(\mathbf{r}, t)$ versus $(-\chi(\mathbf{r}, t))$ plots and time evolution of several time-dependent density functionals. On the other hand, both wave and particle pictures are made use of for the complete description of a physical system in QTM[1,2], in the sense of classical interpretation of quantum mechanics[23] as developed by de Broglie and Bohm. The wave motion is governed by the time-dependent Schrödinger equation (TDSE), while the particle motion is characterized by the velocity defined in terms of gradient of the phase of the wave function. Phase-space distance between two initially closed Bohmian trajectories and the associated Kolmogorov–Sinai (KS) entropy provide important insights into quantum domain chaotic dynamics[11–14]. Behaviour of a single-well oscillator in the presence of an oscillating electric field has also been studied[24] using QTM.

In the present work QTM is applied in analysing the quantum analogue of the KAM transition from a toroidal motion to a chaotic motion associated with the penetration of a barrier in a double-well potential in the presence of a monochromatic external field with increasing amplitude. A theoretical background of the present work is given first followed by computational details. Then results and discussion and some concluding remarks are presented.

The classical Hamiltonian of a double-well oscillator under the influence of an external oscillating driving force is given by

$$H = \frac{p^2}{2m} + ax^4 - bx^2 + gx\cos(\omega_0 t). \quad (1)$$

This Hamiltonian has been used as a mathematical model in understanding many physico-chemical problems such as buckled beam[25], plasma oscillations[26], inversion of pyramidal molecules like ammonia or phosphine[27], hydrogen transfer in atoms and molecules along chemical bonds[28], transport of hydrogen isotopes or muons between interstitial sites in metals[29], macroscopic quantum coherence phenomena in SQUIDS[30], etc. For a given set of parameter values, the classical Hamilton's equations of motion can be solved[12,18,19] to generate the phase-space trajectories. The nature of the phase space depends on initial position and momentum values and one may obtain stable regions in phase space bounded by KAM surfaces or a chaotic sea extended over the whole phase space.

The above classical Hamiltonian is directly quantized in order to get a quantum mechanical description of this problem. The pertinent TDSE can be written as (in au)

*For correspondence. (e-mail: pkc@chem.iitkgp.ernet.in)

$$\hat{\mathbf{H}}\psi(x,\ t)=\left[-\frac{1}{2}\frac{\mathrm{d}^2}{\mathrm{d}x^2}+ax^4-bx^2+gx\cos(\omega_0 t)\right]\psi(x,t)$$

$$=i\frac{\partial\psi(x,t)}{\partial t}, \tag{2}$$

and the velocity which governs the motion of a point particle guided by the wave is given by

$$\dot{\mathbf{x}}=\nabla\chi\ (x,\ t)|_{x=x(t)}, \tag{3}$$

where χ is the velocity potential which appears as the phase of the wave function written in the following polar form:

$$\psi(x,\ t)=\rho^{1/2}(x,\ t)\ \exp[i\chi(x,\ t)]\ . \tag{4}$$

Now, an ensemble of particle motions guided by the same wave can be constructed by varying initial positions

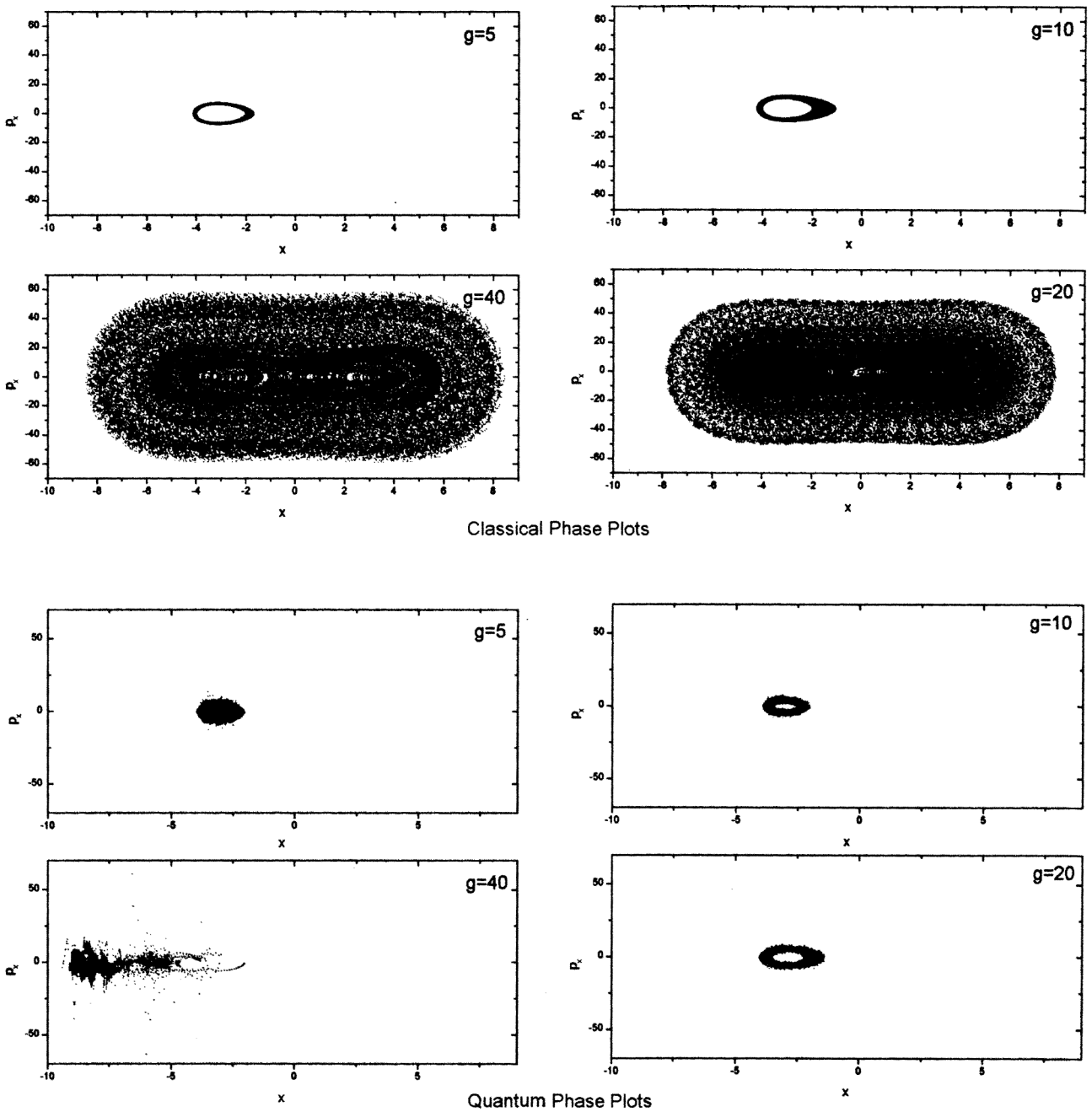

Figure 1. Classical and quantal phase space trajectories for a double-well oscillator in the presence of an external field with g = 5, 10, 20 and 40 with initial condition x_0 = – 2.0 and p_0 = 0.0. Parameter values are: a = 0.5, b = 10.0 and ω_0 = 6.07.

in such a way that the probability of the particle being in this ensemble between x and $x + dx$ at a time t is given by[1] $\rho(x, t)dx$, where $\rho(x, t)$ is $|\psi(x, t)|^2$. Solution of eq. (3) with various initial positions would yield the so-called 'Bohmian trajectories'. In order to study the quantum signature of chaos through sensitive dependence on initial conditions, a phase space distance function[11,13] can be defined as

$$D(t) = [(x_1(t) - x_2(t))^2 + (p_{x_1}(t) - p_{x_2}(t))^2]^{1/2}, \quad (5)$$

where (x, p_x) refers to a point in phase space.

A generalized quantum Lyapunov exponent has also been defined as follows[13] in the same spirit as in classical dynamics,

$$\Lambda = \lim_{\substack{D(0)\to 0 \\ t\to\infty}} \frac{1}{t} \ln\left[\frac{D(t)}{D(0)}\right]. \quad (6)$$

Corresponding KS entropy can be defined as[13]

$$\mathbf{H} = \sum_{\Lambda_+ > 0} \Lambda_+ . \quad (7)$$

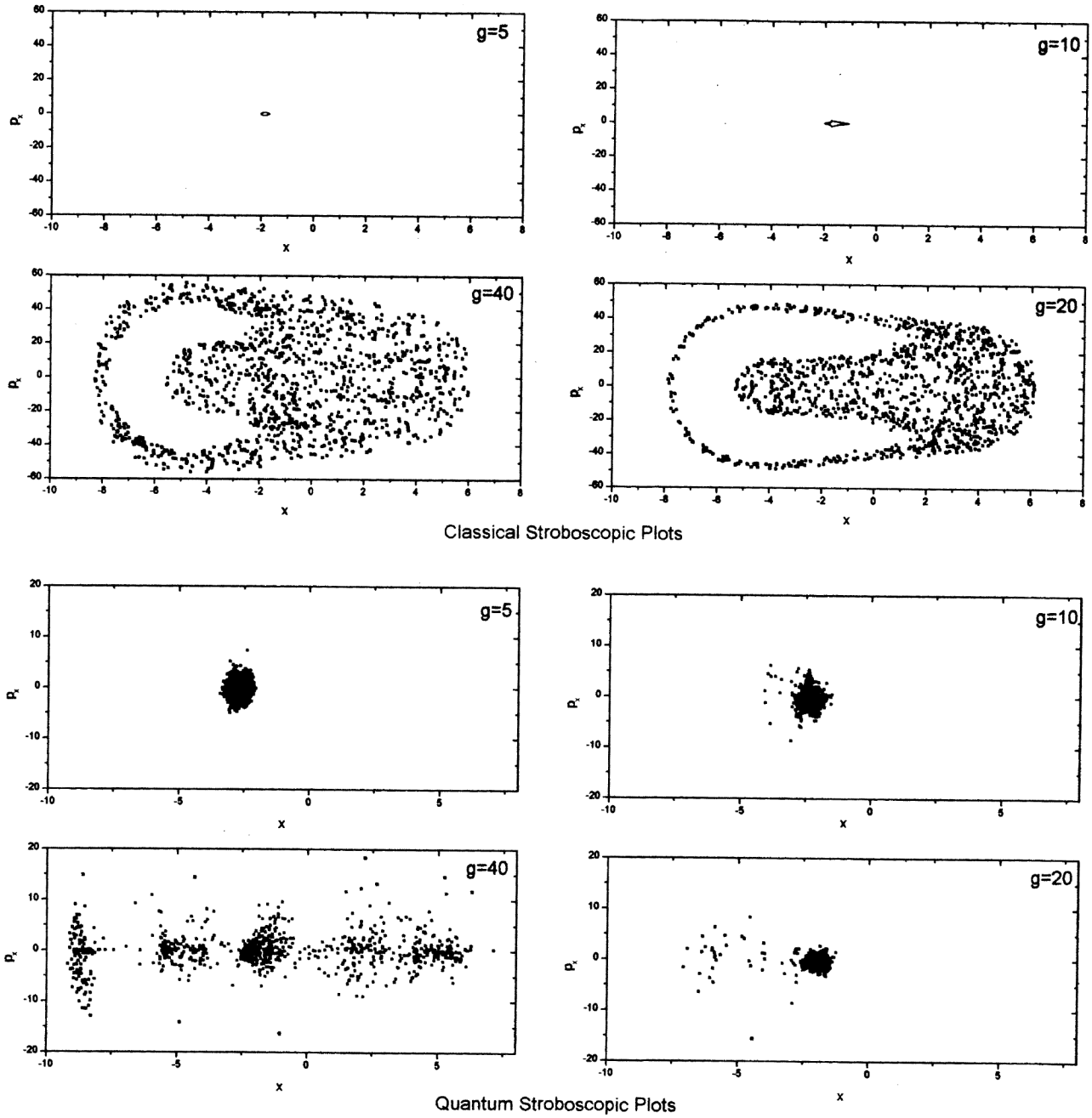

Figure 2. Classical and quantal stroboscopic plots for a double-well oscillator in the presence of an external field. See caption of Figure 1 for details.

Chaotic quantum dynamics is characterized by a positive KS entropy[13].

The phase space volume is defined as[15]

$$V_{ps}(t) = [\langle (x - \langle x \rangle)^2 \rangle \langle (p_x - \langle p_x \rangle)^2 \rangle]^{1/2}. \quad (8)$$

A sharp increase in V_{ps} implies a chaotic motion[12,15]. This quantity is same as the associated uncertainty product which can be used as a measure of quantum fluctuations[18,19]. Classical chaos generally enhances quantum fluctuations[12,15,18,19].

The double-well potential used in the present problem is given by

$$V(x, t) = ax^4 - bx^2 + gx \cos(\omega_0 t), \quad (9)$$

where the parameter values are taken as follows[16]: $a = 0.5$, $b = 10.0$ and $\omega_0 = 6.07$ with initial condition $(x, p_x)|_{t=0} = (-2.0, 0.0)$. In order to understand the breakdown[19] of KAM tori with increasing amplitude of the external field and a possible quantum suppression of the classical chaos, four different g values, viz. $g = 5$, 10, 20 and 40 comprising a completely integrable to a strongly chaotic classical dynamics, are considered. In order to have a better understanding of the behaviour of the system when it goes from subbarrier to superbarrier situations we have also studied the QTM of the various cases studied by Reichl and Zheng[19]. For the sake of completeness, we also generate the classical 'bifurcatio
and its quantum analogue for the quartic oscillator with $a = 1.0$, $b = 8.0$ and $\omega_0 = 6.07$ with the initial condition $(x, p_x)|_{t=0} = (-2.0, 0.0)$, which corresponds to a stable fixed point for this set of parameter values. To understand the classical regular/chaotic motion associated with the field-induced barrier penetration in a quartic potential, the relevant classical Hamilton's equations of motion are solved using a fourth-order Runge–Kutta method up to 10^5 time-steps.

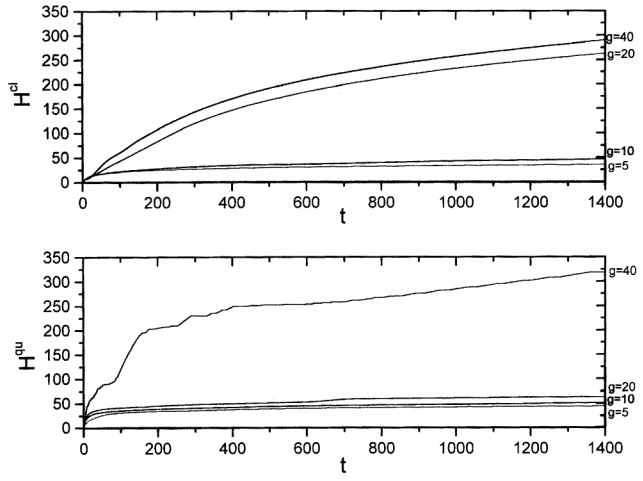

Figure 3. Time evolution of classical (H^{cl}) and quantal (H^{qu}) KS entropies for a double-well oscillator in presence of external field. See caption of Figure 1 for details.

The numerical solution for the quantum dynamics problem starts with the propagation of a Gaussian wave packet under the influence of the quartic potential. For this purpose the pertinent TDSE (eq. (2)) is solved to monitor the temporal evolution of $\psi(x, t)$ using a Peaceman–Rachford-type finite difference algorithm with the Cayley form of the associated unitary operation[31–33]. The details of the numerical technique are available elsewhere[31–33]. The algorithm used here is stable[34] because of the presence of $i = \sqrt{-1}$. As a further check of the numerical accuracy of the scheme, we have verified the conservation of the norm and the energy as well as the reproduction of the initial wave packet through forward propagation up to the end of the simulation followed by back evolution[15]. Mesh sizes adopted are $\Delta x = 0.1$ and $\Delta t = 0.02$. Calculation is carried out for $-15 \le x \le 15$ and for 10^5 time-steps.

Once $\psi(x, t)$ is obtained at a time t, eq. (3) can be rewritten as

$$\dot{\mathbf{x}} = \nabla\chi\ (x, t)|_{x=x(t)} = \mathrm{Re}\left[-\frac{i\nabla\psi}{\psi}\right], \quad (10)$$

which is solved using a second-order Runge–Kutta method to generate the Bohmian trajectories.

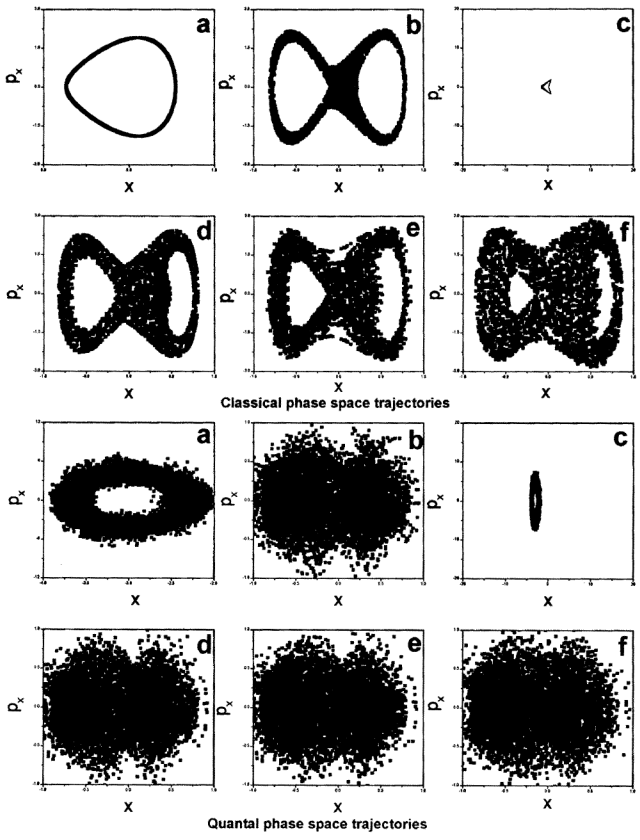

Figure 4. Classical and quantal phase space trajectories for a double-well oscillator in presence of external field with $g = 0.01$, 0.10, 0.18, 0.20, 0.25 and 0.40 with initial condition $x_0 = 0.24$ and $p_0 = 0.0$. Parameter values are $a = 1.0$, $b = 2.0$, $m = 2$ and $\omega_0 = 1.92$.

Figure 1 depicts the classical and quantal phase plots for the four cases with $g = 5$, 10, 20, 40, while the corresponding stroboscopic plots are presented in Figure 2. The classical dynamics is regular for $g = 5$ and 10 and chaotic for $g = 20$ and 40. The first two cases refer to the invariant KAM tori which break down[35,36] for the last two cases to open a pathway in the phase space, allowing a fraction of the particles to migrate from one well to the other over the top of the potential barrier[19]. The presence of both the wells in the phase space structures of $g = 20$ and 40 is transparent. For the quantum variant a robust coherence has already been identified, which results from the interplay between a typical quantal phenomenon like tunnelling and classical chaos that is also amenable to experiments[16]. Although there is an intervening chaotic zone, the wave packet initially launched in one of the wells gradually leaks into the chaotic zone and reaches the other well and eventually oscillates between two 'stability tubes' in a coherent fashion. It has also been shown[37] that for a specific set of parameter values in eq. (2) quantum tunnelling can be completely suppressed and the wave packet would be localized in one of the potential wells. Classical chaos enhances quantum diffusion, but at the same time quantum nonclassical effects suppress classical stochasticity. It appears that a cantorus-like structure[38] is a quantum equivalent of a classical KAM torus. We have not noticed any cantorus-like structure in the underlying classical dynamics. The cantorus structure of the quantum phase space for $g = 20$ is an unmistakable signature of quantum suppression of classical chaos, since the classical KAM torus already breaks down at this strength of the external field. Both these aspects are mimicked by the corresponding KS-entropy plots presented in Figure 3. The case with $g = 40$ is associated with very large KS entropy for both classical and quantum dynamics, implying the effect of classical chaos in enhancing quantum stochasticity. But the H^{cl} for $g = 20$ lies closer to that for $g = 40$, while the H^{qu} for $g = 20$ lies closer to that for $g = 10$, reflecting the quantum suppression of chaos. Autocorrelation function and its power spectrum and the nearest-neighbour spacing distribution (not shown here) lend additional support.

Reichl and Zheng[19] have studied the penetration of the barrier in a double-well potential in the presence of an external field with different amplitudes. We have studied the QTM of all the six cases (*a* to *f*) presented by them for the external field with frequency = 1.92, mass of the particle = 2 and amplitude = 0.01, 0.10, 0.18, 0.20, 0.25 and 0.40. As the field amplitude increases, for a given frequency, the particle originally trapped in one of the wells escapes the barrier.

Figure 4 presents the classical and quantal stroboscopic plots for various field strengths. The external field with very small amplitude (case *a*) has hardly any effect on the particle and it does not escape the well. In case *b* with slightly larger amplitude, particles with energy greater than a specific value can cross the barrier. However, further increase in amplitude (case *c*) resulted in trapping of the particle in a quasiperiodic orbit, a part of which lies above the barrier and a part below it. In cases *d* to *f* we see the increasingly chaotic behaviour with a gradual increase in the field amplitude. For the quantal versions of cases *a* and *c* two cantorus-like structures reaffirm the correspondence between a classical torus and a quantum 'cantorus'.

Figure 5 presents the classical and quantal KS entropies for the cases studied. The relative order is $a < c < b < d < e < f$ for both H^{cl} and H^{qu}, as expected. The plot of the phase volume[15] (or the uncertainty product) which is a measure of quantum fluctuations[18,19] is depicted in Figure 6. This quantity mimicks the above behaviour.

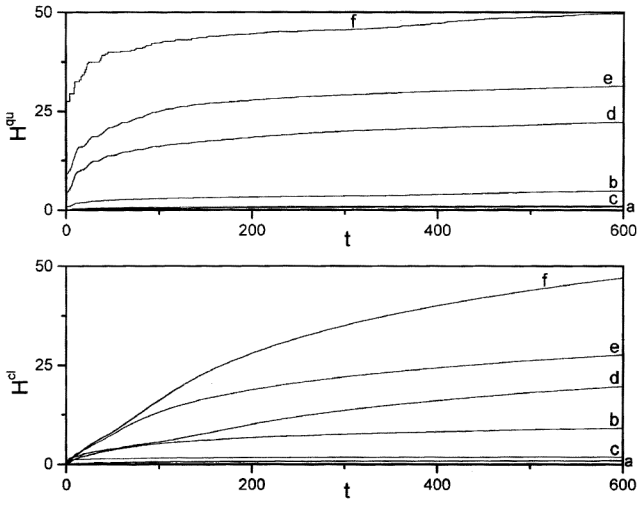

Figure 5. Time evolution of classical (H^{cl}) and quantal (H^{qu}) KS entropies for a double-well oscillator in presence of external field. See the caption of Figure 4 for details.

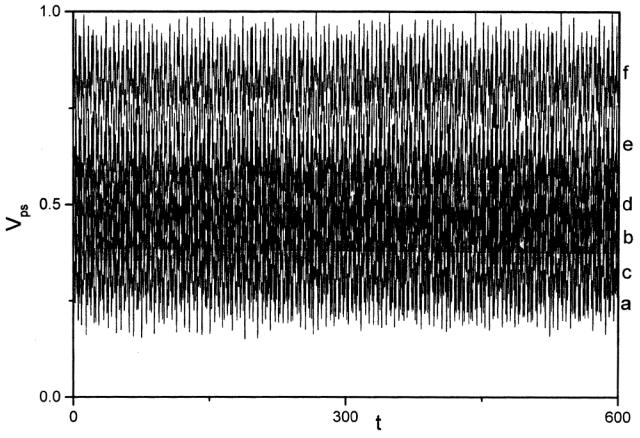

Figure 6. Time evolution of phase space volume (V_{ps}) or the uncertainty product associated with the quantal motion of a double-well oscillator in presence of external field. See the caption of Figure 4 for details.

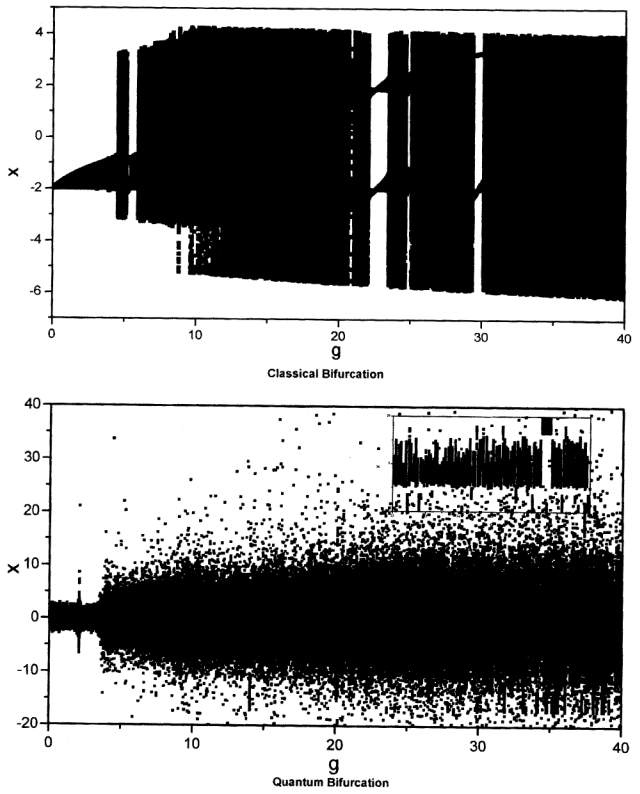

Figure 7. Classical bifurcation diagram and its quantum analogue for a double-well oscillator in presence of external monochromatic field of varying amplitude (g). Parameter values are $a = 1.0$, $b = 8.0$ and $\omega_0 = 6.07$. Initial condition is $x_0 = -2.0$ and $p_0 = 0.0$.

A 'classical bifurcation' diagram for a slightly different set of parameter values ($a = 1.0$, $b = 8.0$ and $\omega_0 = 6.07$) for the double-well oscillator with increasing strength of the external field and its quantum analogue are presented in Figure 7. Difference in width for small g values in classical and quantum cases is due to the respective motions on torus and 'cantorus'. Overall, chaotic classical dynamics goes along with the corresponding chaotic quantum dynamics. Periodic windows in the classical diagram are generally of larger width, but the number of such windows (zoomed portion in inset) is much larger in the quantum case possibly stemming from the suppression of classical chaos by quantum non-classical effects. A part of this work was published earlier[12].

Quantum theory of motion provides important insights into the quantum manifestations of the classical regular and chaotic dynamics of a quartic oscillator in the presence of an external field of different strengths. The classical KAM tori break down at a strength for which the quantal phase portrait still exhibits cantorus-type regular islands owing to the quantum suppression of the classical chaos. It has also been observed that the classical chaos generally enhances typical quantum features like quantum fluctuations. The KS entropy and the uncertainty product support these results.

1. Holland, P. R., *The Quantum Theory of Motion*, Cambridge University Press, Cambridge, 1993.
2. Gutzwiller, M. C., in *Chaos in Classical and Quantum Mechanics*, Springer, Berlin, 1990.
3. Eckhardt, B., *Phys. Rep.*, 1988, **163**, 205–209.
4. Jensen, R. V., *Nature*, 1992, **355**, 311–317.
5. Casati, G., Chirikov, B. V., Shepelyansky, D. L. and Guarneri, I., *Phys. Rev. Lett.*, 1986, **57**, 823–826.
6. de Polavieja, G. G., *Phys. Lett. A*, 1996, **53**, 2059–2061.
7. Frisk, H., *ibid*, 1997, **227**, 139.
8. Konkel, S. and Makowski, A. J., *ibid*, 1998, **238**, 95–100.
9. Nakamura, K. and Lakshmanan, M., *Phys. Rev. Lett.*, 1986, **57**, 1661–1664.
10. Chattaraj, P. K. and Sengupta, S., *Phys. Lett. A*, 1993, **181**, 225–231.
11. Sengupta, S. and Chattaraj, P. K., *ibid*, 1996, **215**, 119–127.
12. Chattaraj, P. K., Sengupta, S. and Podder, A., *Curr. Sci.*, 1999, **76**, 1371–1376.
13. Schwengelbeck, U. and Faisal, F. H. M., *Phys. Lett. A*, 1995, **199**, 281–286.
14. Faisal, F. H. M. and Schwengelbeck, U., *ibid*, 1995, **207**, 31–36.
15. Feit, M. D. and Fleck, Jr. J. A., *J. Chem. Phys.*, 1984, **80**, 2578–2584.
16. Lin, W. A. and Ballentine, L. E., *Phys. Rev. Lett.*, 1990, **65**, 2927–2928.
17. Lakshmanan, M. and Murali, K., *Chaos in Nonlinear Oscillators*, World Scientific, Singapore, 1996.
18. Graham, R. and Hohnerbach, H., *Phys. Rev. A*, 1991, **43**, 3966–3981; Chaudhuri, S., Gangopadhyay, G. and Ray, D. S., *Indian J. Phys. B*, 1995, **69**, 507–523.
19. Reichl, L. E. and Zheng, W. M., *Phys. Rev. A*, 1984, **29**, 2186–2193.
20. McKay, R. S. and Meiss, J. D., *ibid*, 1988, **37**, 4702–4706.
21. Hanggi, P., in *Activated Barrier Crossing* (eds Fleming, G. R. and Hanggi, P.), World Scientific, Singapore, 1993.
22. Madelung, E., *Z. Phys.*, 1926, **40**, 322–326.
23. de Broglie, L., *C. R. Acad. Sci.*, 1926, **183**, 447–448; Bohm, D., *Phys. Rev.*, 1952, **85**, 166–179.
24. Sengupta, S., Poddar, A. and Chattaraj, P. K., *Indian J. Chem. A*, 2000, **39**, 316–322.
25. Moon, F. C., *Chaotic and Fractal Dynamics*, John Wiley, New York, 1985.
26. Guckenhimer, J. and Holmes, P., *Nonlinear Oscillations: Dynamical Systems and Bifurcations of Vector Fields*, Springer-Verlag, New York, p. 1083; Moon, F. C. and Holmes, P. J., *J. Sound Vib.*, 1979, **65**, 275; Holmes, P. J., *Philos. Trans. R. Soc. London*, 1979, **292**, 420.
27. Hund, F., *Z. Phys.*, 1927, **43**, 803.
28. Skinner, J. L. and Trommsdorff, H. P., *J. Chem. Phys.*, 1988, **89**, 897; Oppenländer, A., Rambaud, Ch., Trommsdorff, H. P. and Vial, J. C., *Phys. Rev. Lett.*, 1989, **63**, 1432.
29. Kondo, J., *Physica B (Amsterdam)*, 1984, **125**, 279 and 1984, **126**, 377; Grabert, H., Linkwitz, S., Dattagupta, S. and Weiss, U., *Europhys. Lett.*, 1986, **2**, 631; Wipf, H., Steinbinder, D., Neumair, K., Gutsmiedl, P., Magerl and Dianoux, A. J., *ibid*, 1987, **4**, 1379; Grabert, H. and Wipf, H., in *Festkörperprobleme – Advances in Solid State Physics*, Vieweg, Braunschweig, 1990, vol. 30, p. 1.
30. Tesche, C. D., *Ann. N. Y. Acad. Sci.*, 1986, 480, 36; *Phys. Rev. Lett.*, 1990, **64**, 2358.
31. Goldberg, A., Schey, H. M. and Schwartz, J. L., *Am. J. Phys.*, 1967, **35**, 177–186.
32. Galbraith, I., Ching, Y. S. and Abraham, E., *ibid*, 1984, **52**, 60–68.
33. Chattaraj, P. K., Sengupta, S. and Poddar, A., *Curr. Sci.*, 1998, **74**, 758–764.
34. Chattaraj, P. K., Rao, K. S. and Deb, B. M., *J. Comput. Phys.*, 1987, **72**, 504–512.

35. Chirikov, V., *Phys. Rep.*, 1979, **52**, 263–379.
36. Walker, L. H. and Ford, J., *Phys. Rev.*, 1969, **188**, 416–432.
37. Grossmann, F., Dittrich, T., Jung, P. and Hänggi, P., *Phy. Rev. Lett.*, 1991, **67**, 516–519.
38. McKay, R. S. and Meiss, J. D., *Phys. Rev. A*, 1988, **37**, 4702–4706; Hanson, J. D., Cary, J. R. and Meiss, J. D., *J. Stat. Phys.*, 1985, **39**, 327–345.

ACKNOWLEDGEMENTS. We thank CSIR, New Delhi for financial assistance and a referee for constructive criticism.

Received 18 September 2001; revised accepted 28 January 2002

Pyrethroid resistance in *Anopheles culicifacies* in Surat district, Gujarat, west India

O. P. Singh, K. Raghavendra, N. Nanda, P. K. Mittal and S. K. Subbarao*

Malaria Research Centre (ICMR), 22 Sham Nath Marg, Delhi 110 054, India

A focus of deltamethrin resistance in *Anopheles culicifacies*, the major vector of malaria in India, was identified in Surat district, Gujarat, western coast of India, where two synthetic pyrethroids, deltamethrin and cyfluthrin are being used under the public health programme since 1996, as a selective vector control measure. The per cent mortalities in *An. culicifacies* after one-hour exposure to 0.05% deltamethrin varied from 60 to 78 and LT_{50} and LT_{90} values were 27 to 38 and 164 to 218 min, respectively in different localities; whereas laboratory-maintained pyrethroid susceptible strains showed 100% mortality even at exposure for 10 min. The population also showed high knock-down resistance against 0.05% deltamethrin; the knock-down times, KDT_{50} and KDT_{90}, were 74–81 and 217–297 min respectively as against 8.8–10.7 and 14.2–15.7 min respectively in pyrethroid-susceptible, laboratory-colonized strains of *An. culicifacies* species B and C. The *An. culicifacies* population in the study area was found to comprise of two sibling species, B and C, which did not differ in knock-down susceptibility to deltamethrin.

ANOPHELES culicifacies is a principal vector of malaria in rural and peri-urban areas of India, which alone contributes 60–65% of new malaria cases each year[1]. *An. culicifacies* complex is comprised of five sibling species provisionally designated as A, B, C, D and E[2,3]. Distinct biological variations exist between members of the complex, of which the most important from vector-control point of view are differences in their role in malaria transmission[3–5], susceptibility to malaria infection[6,7], and response to insecticides[8–10]. The main strategy of control of *An. culicifacies* in rural areas is indoor spraying of residual insecticides. Spraying of DDT and HCH under the public health programme was introduced in the 1950s. A few years after the introduction of these insecticides, *An. culicifacies* developed resistance to DDT[11,12], dieldrin[13] and BHC[14]. As a result, malathion was introduced in Gujarat and Maharashtra in 1969 against which *An. culicifacies* developed resistance rapidly by 1973 (ref. 15). Later this species was reported to be triple-resistant in Gujarat, Andhra Pradesh and Haryana[9,10]. As a result, synthetic pyrethroids (SPs) were introduced in some parts of India in the 1990s for selective control of the multiple insecticide-resistant malaria vector/s in high-risk areas.

Gujarat is one of the highly malarious states in India, with Surat district responsible for the maximum number of malaria cases among all districts of the state. In Gujarat *An. culicifacies* has developed resistance to all insecticides used earlier, namely DDT, HCH and malathion[9]. SPs were therefore introduced in some areas of Gujarat with high malaria risk, including Surat district in 1996 as a selective malaria vector-control measure. The present study was undertaken in Surat district to monitor the status of pyrethroid resistance in *An. culicifacies*.

Surat district is situated on the western coast of India between 21–22°N latitude and 73–74°E longitude. Villages under three Primary Health Centres (PHC) of two talukas (sub-division of district) of Surat district which have different history of insecticide selection pressure, were selected for the study. The study area is predominantly hilly and forested. *An. culicifacies* is the predominant species among anophelines and is the main malaria vector in the area. The study villages and history of insecticides used in these villages since 1995 are given in Table 1. Under Amladam PHC, all 29 villages are under indoor residual spraying of cyfluthrin/deltamethrin since 1996, whereas in other PHCs, villages with higher malaria risk are covered with these insecticides.

To monitor the susceptibility status, indoor resting *An. culicifacies* females were collected from the study villages in the morning (6–8 a.m.) using an aspirator and torch light. Blood-fed mosquitoes were exposed to 0.05% deltamethrin-impregnated paper, a revised diagnostic dose recommended by WHO[16], using standard WHO's adult susceptibility test kit for 5, 10, 15, 30, 60, 120 and 240 min, and were held for 24 h recovery period with access to cotton pad soaked with 5% glucose solution in water. Mortality was recorded after 24 h recovery. Corrected per cent mortalities (using Abbott's formula) after 1 h exposure and 24 h holding were used for assessing resistance status. To determine knock-down susceptibility,

*For correspondence. (e-mail: sks2000@vsnl.com)